International Journal of Pharmaceutics 621 (2022) 121809

Contents lists available at ScienceDirect

International Journal of Pharmaceutics

journal homepage: www.elsevier.com/locate/ijpharm

Zein-polycaprolactone core–shell nanofibers for wound healing

Alma Martin [a,b], Jun Cai [a], Anna-Lena Schaedel [a], Mariena van der Plas [a,c], Martin Malmsten [a,d], Thomas Rades [a], Andrea Heinz [a,*]

[a] LEO Foundation Center for Cutaneous Drug Delivery, Department of Pharmacy, University of Copenhagen, 2100 Copenhagen, Denmark
[b] School of Medicine, Nazarbayev University, 010000 Nur-Sultan, Kazakhstan[1]
[c] Division of Dermatology and Venereology, Department of Clinical Sciences Lund, Lund University, S-22184 Lund, Sweden
[d] Department of Physical Chemistry, Lund University, S-221 00 Lund, Sweden

ARTICLE INFO

Keywords:
Biomaterial
Coaxial electrospinning
Sustained release
Tissue regeneration

ABSTRACT

In a previous study, we developed electrospun antimicrobial microfiber scaffolds for wound healing composed of a core of zein protein and a shell containing polyethylene oxide. While providing a promising platform for composite nanofiber design, the scaffolds showed low tensile strengths, insufficient water stability, as well as burst release of the antimicrobial drug tetracycline hydrochloride, properties which are not ideal for the use of the scaffolds as wound dressings. Therefore, the aim of the present study was to develop fibers with enhanced mechanical strength and water stability, also displaying sustained release of tetracycline hydrochloride. Zein was chosen as core material, while the shell was formed by the hydrophobic polymer polycaprolactone, either alone or in combination with polyethylene oxide. As compared to control fibers of pristine polycaprolactone, the zein-polycaprolactone fibers exhibited a reduced diameter and hydrophobicity, which is beneficial for cell attachment and wound closure. Such fibers also demonstrated sustained release of tetracycline hydrochloride, as well as water stability, ductility, high mechanical strength and fibroblast attachment, hence representing a step towards the development of biodegradable wound dressings with prolonged drug release, which can be left on the wound for a longer time.

1. Introduction

With an increase of the aging population as well as chronic health conditions such as diabetes and obesity, wound care, alongside the economic burden it generates, has evolved into a major public health concern (Olsson et al., 2019). Wound dressings play a vital role in the treatment of wounds and have to meet a number of criteria to provide a favorable environment for wound closure and tissue regeneration. These criteria include absorbing excess exudate, maintaining a moist healing environment, protecting the wound from microorganisms and infection, and facilitating gas exchange as well as cell migration and attachment. The dressing material should further be non-toxic and biocompatible (Azimi et al., 2020; Liu et al., 2021). In terms of mechanical properties, a wound dressing should be elastic and ductile in order to allow easy

Abbreviations: AA, acetic acid; DL, drug loading; ECM, extracellular matrix; EDTA, ethylenediaminetetraacetic acid; EE, encapsulation efficiency; EMA, European Medicines Agency; FDA, Food and Drug Administration; LB, Luria-Bertani; LDH, lactate dehydrogenase; MDSC, modulated differential scanning calorimetry; MQ, Milli-Q deionized water; MTT, 3-(4,5-dimethylthiazol-2-yl)-2,5-diphenyltetrazolium bromide; NFM, nanofiber mat; OD, optical density; PBS, phosphate-buffered saline; PCL, polycaprolactone; 25PCL, fibers composed of pristine polycaprolactone; PEO, polyethylene oxide; RT, room temperature; SD, standard deviation; SEM, scanning electron microscopy; T, tetracycline hydrochloride; TDL, theoretical drug loading; T25PCL, fibers composed of pristine polycaprolactone and tetracycline hydrochloride; XRD, X-ray diffraction; zein-25PCL, core–shell fibers containing zein in the core and 25 % PCL in the shell; zeinT-25PCL, core–shell fibers containing zein and tetracycline hydrochloride in the core and 25 % PCL in the shell; zein-1PEO/1PCL, core–shell fibers containing zein in the core and 1 % PEO as well as 1 % PCL in the shell; zeinT-1PEO/1PCL, core–shell fibers containing zein and tetracycline hydrochloride in the core and 1 % PEO as well as 1 % PCL in the shell; zein-1PEO/3PCL, core–shell fibers containing zein in the core and 1 % PEO as well as 3 % PCL in the shell; zeinT-1PEO/3PCL, core–shell fibers containing zein and tetracycline hydrochloride in the core and 1 % PEO as well as 3 % PCL in the shell.

* Corresponding author at: University of Copenhagen Department of Pharmacy, LEO Foundation Center for Cutaneous Drug Delivery Universitetsparken 2 2100 Copenhagen Denmark.
E-mail address: andrea.heinz@sund.ku.dk (A. Heinz).
[1] Current address.

https://doi.org/10.1016/j.ijpharm.2022.121809
Received 16 March 2022; Received in revised form 28 April 2022; Accepted 5 May 2022
Available online 10 May 2022

handling and comfortable wear, and it should have a sufficiently high mechanical strength to be unaffected by tear. Lastly, it should not adhere to the wound to allow painless removal and exchange (Azimi et al., 2020). Different types of wound dressings are available on the market, including films (Moreira et al., 2021), foams (Trucillo and Di Maio, 2021), sponges (Pachuau, 2015), hydrogels (Op 't Veld et al., 2020), as well as fiber-based scaffolds (Azimi et al., 2020; Liu et al., 2021). Among these, nanofiber scaffolds prepared by electrospinning have gained increasing significance as their microstructure and mechanical properties can be tuned to resemble those of extracellular matrix (ECM) proteins (Azimi et al., 2020; Memic et al., 2019). Moreover, their high porosities and small pore sizes facilitate gas exchange as well as fibroblast and keratinocyte migration and attachment, thereby enhancing ECM remodeling and wound closure (Azimi et al., 2020; Liu et al., 2021; Memic et al., 2019). Additionally, due to their high surface areas and adaptable morphologies, drug release properties of the fibers can be tailored to meet the specific requirements of different types of wounds (Feng et al., 2019).

Electrospinning is a versatile and robust technique, which allows fabricating micro- and nanofibrous scaffolds with tunable mechanical, drug release and degradation properties from a wide variety of natural and synthetic polymers. The technique is based on the application of high electric voltage to a polymer solution at a needle tip to form a conical shape, the so-called Taylor cone, which in turn generates a jet. The emerged jet stretches under solvent evaporation to form fibers that are deposited on an oppositely charged collector (Luraghi et al., 2021). Among different plant proteins, biocompatible and biodegradable zein is promising for electrospinning of drug delivery systems for tissue regeneration (Labib, 2018; Paliwal and Palakurthi, 2014). Its amphiphilic nature accounts for its solubility in aqueous ethanol, a solvent considered as non-genotoxic and of lower risk to human health according to both the Food and Drug Administration (FDA) and European Medicines Agency (EMA, 2021). However, electrospinning of zein in aqueous ethanol is challenging due to the high evaporation rate of ethanol, which creates a polymer skin on the surface of the polymer solution, leading to clogging and ribbon-shaped fibers (Kanjanapongkul et al., 2010). Moreover, zein fibers tend to swell upon contact with water, leading to a loss of the fibrous structure of the mat. In order to compensate for these unfavorable properties, synthetic co-polymers such as polylactic acid, polyurethane, and polycaprolactone (PCL) have been electrospun together with zein in a uniaxial set-up (Alhusein et al., 2016; Ghorbani et al., 2020; Maharjan et al., 2017), while cross-linking agents such as formaldehyde or glutaraldehyde have been added after electrospinning (Selling et al., 2011; Selling et al., 2008).

In contrast to conventional uniaxial electrospinning, where polymer and co-polymer are blended in one polymer solution, coaxial electrospinning makes use of a core and shell solution (Han and Steckl, 2019). Previously, we have demonstrated that electrospinning of a zein core solution can be facilitated by hydrophilic polyethylene oxide (PEO) in aqueous ethanol as a shell solution (Akhmetova et al., 2020). The zein-PEO core–shell fibers we obtained, however, showed a low mechanical strength, making them susceptible to wear and tear. They further did not fully retain their shape upon absorption of water, decreasing interfibrous porosity and hence, potentially also gas exchange and cell migration. Moreover, we observed a burst release of the incorporated antimicrobial drug tetracycline hydrochloride (T), which would require high changing frequencies of the wound dressing in clinical use (Akhmetova et al., 2020).

Addressing these shortcomings, the aim of the present study was to further develop our fibers to obtain wound dressings with both good ductility and mechanical strength as well as water stability and shape retention. Moreover, we aimed at achieving a sustained T release in order to reduce the changing frequency of a potential wound dressing and to suppress infection over a longer time. For this purpose, we selected the semi-crystalline polymer PCL to either fully replace PEO or to be used in combination with PEO in the fiber shell surrounding the zein core. PCL is a biodegradable polymer approved by the FDA (Janmohammadi and Nourbakhsh, 2019), which has previously been observed to provide sufficient strength and flexibility to wound dressings (Augustine et al., 2015). Not only can PCL be electrospun in glacial acetic acid (AA), a solvent generally recognized as safe by both FDA and EMA (2021), but any traces of residual AA in the fabricated fibers may suppress bacterial infection further due to the antimicrobial properties of AA (Agrawal et al., 2017). There are some studies reporting electrospinning of zein with PCL in a uniaxial (Alhusein et al., 2016; Alhusein et al., 2013; Ghorbani et al., 2020; Pedram Rad et al., 2018), two-nozzle (Pedram Rad et al., 2019) and multilayered (Alhusein et al., 2016; Pedram Rad et al., 2019) fashion as well as by coaxial electrospinning with PCL in the core and zein in the shell (He et al., 2017; Jiang et al., 2007). However, to the best of our knowledge, zein has not been electrospun coaxially with a zein core and PCL shell. Overall, we demonstrate in this study that water stable, ductile, mechanically strong zein-PCL core–shell nanofibers can be produced by coaxial electrospinning using aqueous ethanol and AA as solvents. These nanofibers display sustained release of T, as well as potent antimicrobial activity, and efficient fibroblast attachment. Together, the results obtained for the zein-PCL core–shell nanofibers represent a step towards the development of modern biodegradable wound dressings, which release the active pharmaceutical ingredient in a sustained fashion, decreasing the wound dressings' changing frequency.

2. Materials and methods

2.1. Materials

All materials were obtained from Sigma-Aldrich (Darmstadt, Germany), unless specified otherwise. PEO (~900 kDa) and PCL (~80 kDa) were used as polymers for electrospinning and glacial AA and absolute ethanol (VWR International, as part of Avator, Søborg, Denmark) as solvents. Tetracycline hydrochloride (T, ≥95 % purity) was used as active pharmaceutical ingredient. Antimicrobial susceptibility test discs (30 μg T, Oxoid), Luria-Bertani (LB) broth, Bacto Agar (Saveen & Werner, Limhamn, Sweden), 24-well plate inserts (CellCrown, Scaffdex, Tampere, Finland), 4 % formaldehyde-buffered aqueous solution (VWR International) and MQ water (Reference A +) were used. For the cell study, Medium 106 (Thermo Fisher, Roskilde, Denmark), low serum growth supplement (Thermo Fisher), antibiotic–antimycotic (Thermo Fisher), Dulbecco's phosphate-buffered saline (PBS), trypsin-EDTA solution, trypan blue solution (0.4 %), and 3-(4,5-dimethylthiazol-2-yl)-2,5-diphenyltetrazolium bromide (MTT) were used.

2.2. Preparation of nanofiber mats

Four types of nanofiber mats (NFMs) were electrospun with increasing PCL amounts to study the influence of an increasing PCL amount on the mechanical properties, release properties as well as biological properties of the fiber mats. More specifically, three types of coaxially electrospun core–shell fibers containing zein in the core and PEO and/or PCL (1 %, 3 % or 25 %, respectively) in the shell as well as one type of uniaxially electrospun control sample containing PCL only were produced (Table 1). For the core–shell fibers, the core solution consisted of 20 % (w/v) zein dissolved in 80 % (v/v) aqueous ethanol at 60 °C under continuous stirring for 2 h. For the PCL-based shell solution, 25 % (w/v) PCL was dissolved in glacial AA for 2 h in a sonication bath at 70 °C. For the PEO/PCL-based shell solution, 1 % (w/v) PEO was added to the dissolved 1 % or 3 % PCL (w/v) solution in glacial AA, respectively, and allowed to mix overnight at RT. In the case of drug-loaded fibers, 5 % (w/w of zein) T was added to the zein solution and mixed for 10 min at 60 °C. Additionally, PCL at 25 % (w/v) in glacial AA was electrospun uniaxially. For the drug-loaded PCL fibers, T was added at 2 % (w/w of PCL) due to its limited solubility in glacial AA. The electrospinning settings were selected according to the stability of the

Table 1
Electrospinning solutions, conditions and settings.

Abbreviation	Core (%, w/v)	Shell (%, w/v)	Core flow rate (μL/h)	Shell flow rate (μL/h)	Injector voltage (kV)	Collector voltage (kV)	Distance injector collector (cm)
zein-1PEO/1PCL	20% zein	1% PCL + 1% PEO	500	700	7	−0.8	18
zeinT-1PEO/1PCL	20% zein + 5 % T	1% PCL + 1% PEO	500	700	7	−0.8	18
zein-1PEO/3PCL	20% zein	3% PCL + 1% PEO	500	700	8	−0.8	18
zeinT-1PEO/3PCL	20% zein + 5 % T	3% PCL + 1% PEO	500	700	8	−0.8	18
zein-25PCL	20% zein	25% PCL	100	600	16	−6	25
zeinT-25PCL	20% zein + 5 % T	25% PCL	200	800	13	−6	25
25PCL	25% PCL	None	200	–	6	−1	25
T25PCL	25% PCL + 2 % T	None	200	–	7	−6	25

Taylor cone and the jet (Table 1). All samples were stored at 0 % RH and sterilized with UV light at 254 nm for 2 h on each side before further analysis.

The viscosities of the 20 % (w/v) zein solution in 80 % (v/v) aqueous ethanol and the 25 % (w/v) PCL solution in glacial AA were measured at 22 °C using a AR-G2 Magnetic Bearing Rheometer (TA Instruments Ltd, West Sussex, UK) and a 40 mm cone-plate geometry set-up.

2.3. Fiber diameter and size distribution

Fiber diameter and size distribution of the NFMs were analyzed using scanning electron microscopy (SEM) on a TM3030 (Hitachi, Tokyo, Japan) as described previously (Akhmetova et al., 2020). At least 100 fibers were included in the analysis for each type of NFM.

2.4. Interaction of nanofiber mats with water

Wettability (water contact angle), water stability, water uptake and mass loss were determined after cutting the NFMs into circles of 6 mm diameter. The wettability was analyzed by the sessile drop method for 30 s at RT using a Drop Shape Analyzer (DSA100, Krüss, Hamburg, Germany). For water stability testing, the samples were immersed in water at 37 °C for 48 h, after which the samples were rinsed twice with MQ water and blotted with tissue paper. All samples were then dried at 0 % RH overnight and analyzed using SEM as described previously (Akhmetova et al., 2020). Water uptake by NFMs was studied by recording the initial dry weight of the samples and incubating them with MQ water in a 24-well plate at 37 °C under constant shaking at 200 rpm (neoMix thermoshaker, neoLab, Heidelberg, Germany) for 48 h, after which the NFMs were gently blotted with tissue paper and weighed again. Mass loss of the NFMs was analyzed by determining the change in dry mass before and after 48 h incubation of samples in MQ water. Measurements were conducted in triplicate.

2.5. Mechanical characterization of nanofiber mats

Tensile properties of dry and wetted NFMs were measured at RT on 40 × 10 mm samples using a texture analyzer TA.XT plus (Stable Micro Systems, Godalming, UK) as described previously (Akhmetova et al., 2020). A force of 0.01 N and a speed of 0.5 mm s^{-1} were applied, and experiments were performed in quintuplicate.

2.6. Solid-state characterization of nanofiber mats

NFMs, as well as the individual components forming these, were analyzed with modulated differential scanning calorimetry (MDSC) and X-ray diffraction (XRD). For MDSC analysis on a TA Discovery instrument (New Castle, USA), samples in hermetic pans with pierced lids were subjected to a heat-cool-heat cycle from −10 °C to 230 °C with a modulation amplitude of 0.3180 °C, modulation period of 60 s and a heating rate of 10 °C min^{-1} for the first heating and cooling, and 2 °C min^{-1} during reheating. XRD analysis was carried out on a X'pert PRO (PANanalytical, Malvern, UK) as described previously (Akhmetova et al., 2020).

2.7. Drug loading and release

Drug loading and drug release experiments from NFMs were conducted using sterilized NFM samples cut into circles (6 mm diameter). For drug loading experiments, the NFM samples were dissolved in glacial AA and filtered through a 0.22 μm syringe filter. For release testing, NFM samples were placed into 24 well plates with MQ water at 37 °C under shaking at 200 rpm (neoMix thermoshaker), and release samples were taken out at specific time points. Both, samples of the drug loading and release experiments were analyzed by HPLC (Shimadzu, CTO-20A/20AC, Kyoto, Japan) at 40 °C using a ShimPack GIST C18 column (Shimadzu, Kyoto, Japan) and UV detection at 300 nm as described earlier (Akhmetova et al., 2020).

2.8. Antimicrobial study

Gram-negative *Escherichia coli* (ATCC 25922) and Gram-positive *Staphylococcus aureus* (ATCC 29213) were cultured overnight at 37 °C in LB broth under vigorous shaking. For the agar diffusion test, 0.1 mL of the overnight cultures, diluted to an OD600 of 0.7, were spread evenly over the surface of LB agar plates. Subsequently, dry NFMs of 6 mm in diameter or 30 μg T discs as a control were placed on top of the plates. After 24 h incubation at 37 °C, images of the inhibition zones were recorded with ChemiDoc imaging system (BioRad Laboratories, Copenhagen, Denmark) and analyzed with ImageJ software (1.52a version).

2.9. In vitro cell cultures and wound scratch assay

Primary neonatal human dermal fibroblasts (Invitrogen) were cultured following manufacturer's instructions. For the MTT and lactate dehydrogenase (LDH) assays, 5×10^4 cells in 1 mL were seeded in each well of a 24-well plate and cultured to 90 % confluence. Next, NFMs of 6 mm diameter were placed in the wells, while untreated cells and cells with 30 μL T solution were used as negative and positive controls, respectively, followed by incubation for 24 h at 37 °C and 5 % CO_2.

For the wound scratch assay, cells were prepared as described above

and a scratch was made in the middle of each well with a 200 μL pipette, followed by the addition of the NFMs or 30 μL T solution as described above. For another control, neither NFMs nor T solution were added and only a scratch was made. Images were taken with light microscopy (EVOS, Thermo Fisher) before and after 24 h incubation at 37 °C and 5 % CO_2. The experiment was carried out in duplicate. Cell attachment and migration on the NFMs were investigated after fixing the cells with 4 % formaldehyde for 30 min as described previously (Akhmetova et al., 2020).

2.10. Cell viability assays

LDH release in the cell culture medium was measured using the Pierce LDH Cytotoxicity Assay kit (Thermo Fisher) according to manufacturer's instructions. For the MTT assay, the NFMs were removed and the remaining medium was replaced with 100 μL of fresh medium and 11 μL of MTT solution (5 mg mL^{-1} in PBS); lysed cells were used as a control. After 2–4 h incubation, cells were washed with PBS and 100 μL of dimethyl sulfoxide was added followed by a 10 min incubation at RT and measurement of the absorbance at 550 nm using a VICTOR Nivo plate reader (Perkin Elmer, Skovlunde, Denmark).

2.11. Statistical analysis

DSC data were analyzed using the TRIOS software (TA, New Castle, USA), and the rest of the data were analyzed using OriginPro software (version 9.6.0.172). The data are presented as mean values ± standard deviations at $p < 0.01$ (**), $p < 0.001$ (***) or $p < 0.0001$ (****). One-way analysis of variance followed by Tukey's test was used for comparison of mean values and Levene's test to assess the equality of variances.

3. Results

3.1. Morphology and fiber diameter distribution of nanofiber mats

Different electrospinning settings were tested empirically and artifact-free nanofibers, i.e., fibers free of beads and irregularities, were obtained using the electrospinning settings specified in Table 1. Both drug-loaded and drug-free PEO-containing NFMs (zein-1PEO/1PCL and zein 1PEO/3PCL, Table 1) showed tubular fibers of similar diameters around 900 nm (Fig. 1). Combining a zein core and a PCL shell without PEO and T (zein-25PCL) resulted in a significant decrease ($p < 0.001$) of the fiber diameter to around 600 nm, whereas pristine 25 % (w/v) PCL fiber mats without T (25PCL) showed much larger fiber diameters of ~ 1450 nm. Furthermore, incorporation of T into the zein-25PCL fibers resulted in a bimodal distribution of tubular- and ribbon-shaped fibers. A less pronounced bimodal distribution was observed for pristine 25 % (w/v) PCL fibers electrospun with T (Fig. 1).

Water stability testing, i.e., SEM analysis after incubation of the NFMs in excess MQ water revealed a varying structural stability of the fibers (Fig. 1). Overall, an increase in PCL amount better preserved the shape of single fibers. In contrast, all PEO-containing samples lost their fibrous structure, which is why an analysis of fiber diameter and size distribution was not possible. The drug-loaded zein-25PCL fibers were significantly swollen ($p < 0.001$) after 48 h exposure to water and showed a higher diameter in comparison to their dry state. No significant change in fiber diameter was observed in the uniaxially electrospun zein-free PCL fibers (25PCL) after exposure to water.

3.2. Interaction of the nanofiber mats with water

Wettability analysis revealed that despite the initially high contact angles of all NFMs, water was quickly absorbed within 30 s for many samples, except for the zein-1PEO/1PCL NFMs and the pristine 25PCL

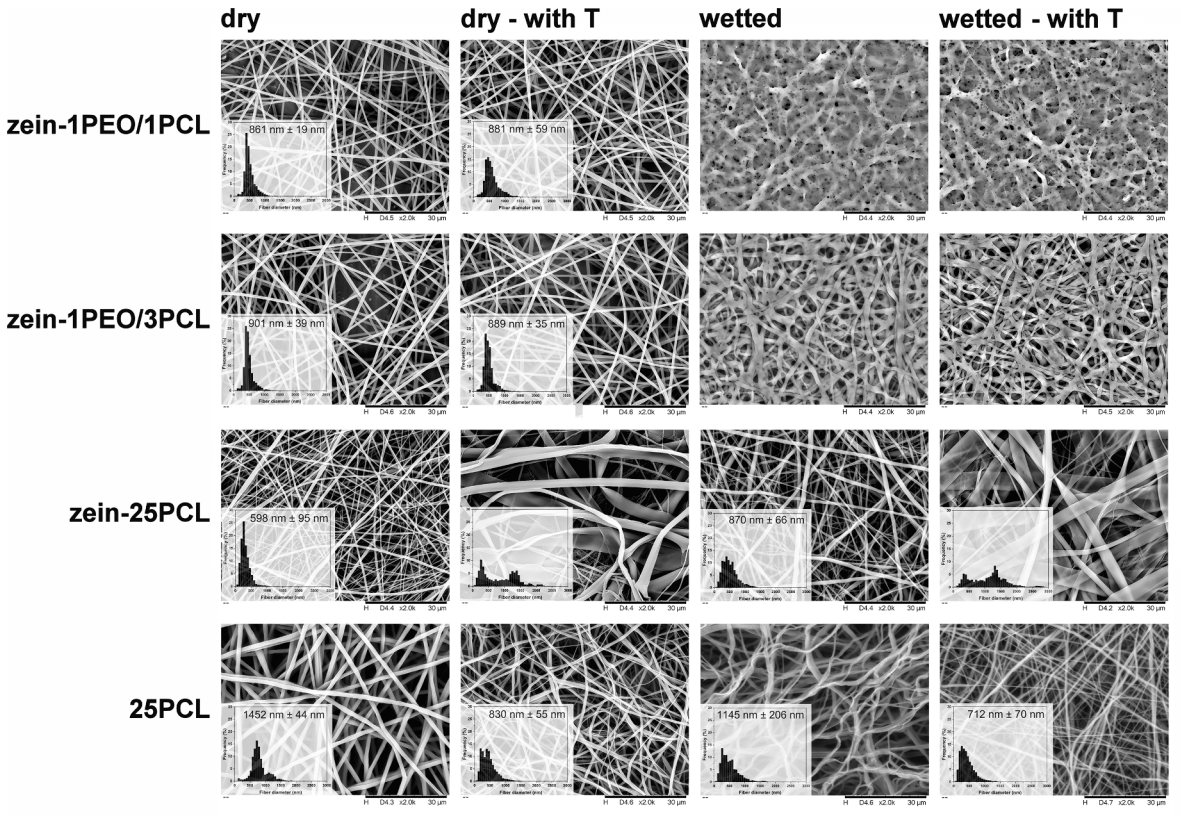

Fig. 1. SEM analysis of the fiber morphology and diameter for zein-1PEO/1PCL, zein-1PEO/3PCL, zein-25PCL, and 25PCL fiber mats freshly prepared and after 48 h exposure to MQ water, respectively. Fiber diameter size distributions are only shown for samples that were possible to analyze with ImageJ.

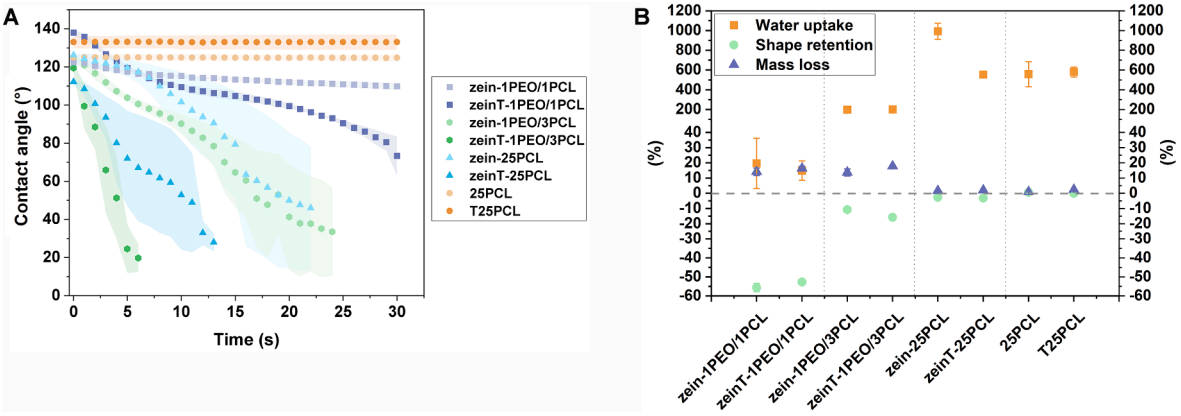

Fig. 2. Interactions of the NFMs with water. (A) Wettability (water contact angle) and (B) comparison between water uptake, mass loss and shape retention of the NFMs.

fibers with and without T. These latter samples remained non-wetted by water, with a contact angle of ~ 125° - 135° (Fig. 2**A**). Irrespective of the PCL concentration, incorporation of T in all samples with a zein core reduced the contact angles as compared to the non-drug-loaded samples.

Water uptake, as well as shape retention and mass loss of the NFMs were studied over 48 h and were found to depend on the PCL concentration (Fig. 2**B**). The zein-1PEO/1PCL NFMs shrunk by approximately 50 % and showed a low water uptake and mass loss (around 15 %), while an increase of the PCL concentration from 1 % to 3 % (w/v) (zein-1PEO/3PCL) resulted in better shape retention of the NFMs and greater water uptake up to 200 %, with the mass loss being unaffected (around 15 %). A further increase of the PCL concentration to 25 % (w/v) (zein-25PCL and 25PCL) reduced the mass loss to approximately 2 % and enhanced the water uptake up to 600 % – 1000 %, while the shape of the NFM was almost fully retained (Fig. 2**B**).

3.3. Mechanical characterization

A significant difference was observed between PEO-containing and PEO-free NFMs regarding both elongation and tensile strength at break (Table 2). When the concentration of PCL was higher than that of PEO, there was a significant increase in elongation and tensile strength. Moreover, with the increase in PCL concentration, the NFMs showed a lower Young's modulus (Table 2) and were more ductile (Fig. 3). In addition, a large difference between dry and wetted state of the PEO-containing NFMs was observed. For instance, the wetted fibers reached an elongation of approximately 140 % in the case of zein-1PEO/3PCL, whilst the dry fibers only showed around 5 % elongation (Table 2). In contrast, no significant difference in the mechanical properties of the dry and wetted states of 25PCL was found (Table 2). All T-loaded core–shell NFMs displayed lower elongation in comparison to their drug-free counterparts irrespective of their composition. In most cases, however, the difference in elongation between samples with and without T was not significant, except for the zein-25PCL samples. Due to the undesired mechanical properties, i.e., low tensile strength and low elongation, of drug-free and drug-loaded zein-1PEO/1PCL samples, these were excluded from further characterization.

3.4. Solid-state characterization

The solid-state properties of the NFMs and their separate constituents were analyzed by MDSC and XRD (Fig. 4). The amorphous nature of zein was confirmed by the diffractograms of the raw material. The thermograms reveal the glass transition temperature (T_g) for pure zein powder at 158.0 ± 0.9 °C, and for zein within the NFMs at around 161.9 ± 1.3 °C (Fig. 4**A**). The melting endotherms for the pure semi-crystalline polymers PCL and PEO were at 56 °C and 65 °C, respectively. The thermograms of the NFMs show separate melting endotherms for PEO and PCL, which is also confirmed by PEO and PCL peaks visible in the XRD diffractograms of the otherwise amorphous material as indicated by the typical halo (Fig. 4**B**).

3.5. Drug loading and release

The actual drug loading of T within all zein-based core–shell fibers was approximately 30 μg per sample, while the drug loading of T25PCL samples was lower (6 μg) due to the solubility limitation of T in the glacial AA (Table 3). Therefore, the latter samples were excluded from further biological experiments. Encapsulation efficiency of T within all NFMs was above 70 % (Table 3). HPLC analysis demonstrated a burst release of T within 20 min from zein-1PEO/3PCL samples and delayed release with increasing PCL concentration (Fig. 5). However, the release

Table 2
Mechanical properties of the dry and wetted NFMs.

Sample	Young's Modulus, kPa		Tensile strength at break, kPa		Elongation at break, %	
	dry ± SD	wet ± SD	dry ± SD	wet ± SD	dry ± SD	wet ± SD
zein-1PEO/1PCL	9.1 ± 1.3	0.4 ± 0.2	150.5 ± 25.6	19.6 ± 4.3	2.7 ± 0.6	61.4 ± 2.5
zeinT-1PEO/1PCL	14.3 ± 4.2	0.2 ± 0.1	211.3 ± 70.2	10.7 ± 2.9	2.3 ± 0.2	40.9 ± 7.3
zein-1PEO/3PCL	9.8 ± 0.5	0.3 ± 0.0	221.1 ± 16.0	19.8 ± 1.0	4.8 ± 0.7	139.8 ± 1.4
zeinT-1PEO/3PCL	8.8 ± 2.5	0.2 ± 0.0	168.3 ± 71.4	21.7 ± 3.7	3.8 ± 0.7	105.8 ± 13.2
zein-25PCL	3.0 ± 1.0	1.9 ± 0.2	475.3 ± 86.0	434.1 ± 55.4	131.7 ± 14.8	116.3 ± 5.6
zeinT-25PCL	1.4 ± 0.7	0.8 ± 0.1	236.4 ± 85.7	180.9 ± 25.3	78.0 ± 9.4	69.6 ± 1.4
25PCL	0.8 ± 0.2	0.6 ± 0.0	372.0 ± 98.6	253.6 ± 50.0	111.0 ± 13.8	89.7 ± 24.0
T25PCL	0.8 ± 0.0	1.2 ± 0.1	370.3 ± 14.2	504.7 ± 35.7	143.7 ± 6.3	114.5 ± 3.7

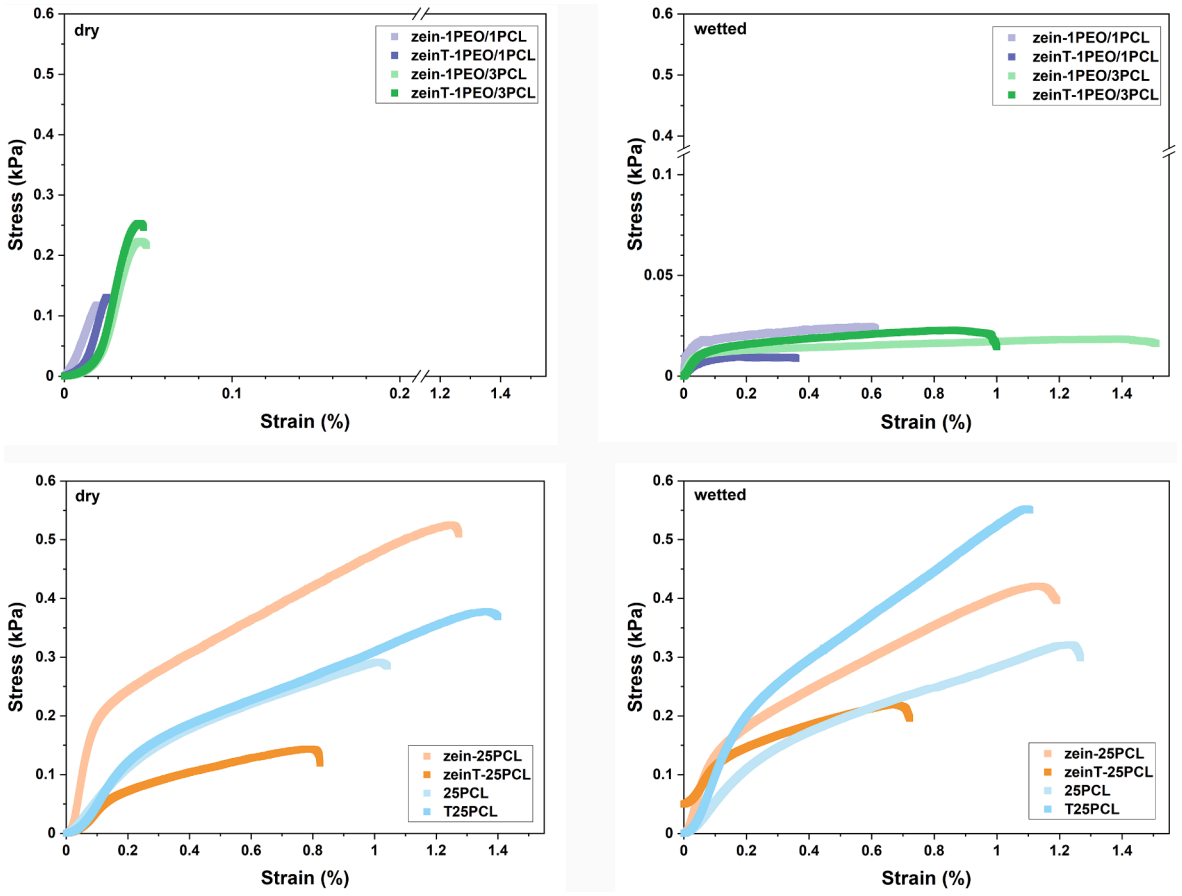

Fig. 3. Strain-stress profiles of the dry (left hand side) and hydrated (right hand side) NFMs.

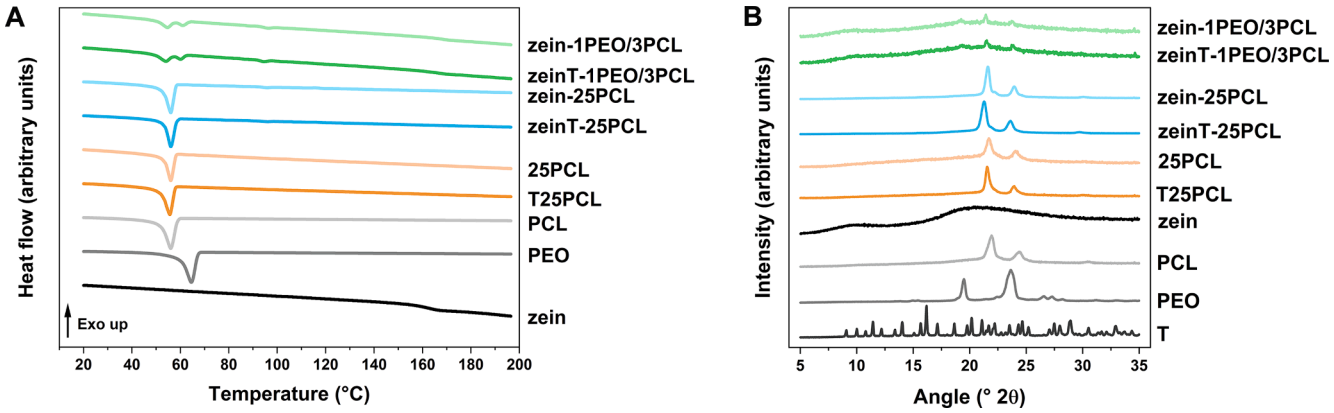

Fig. 4. Solid-state characterization of the NFMs, showing (A) MDSC thermograms and (B) X-ray diffractograms of the NFMs and their individual components, respectively.

Table 3
Encapsulation efficiency and theoretical and actual drug loading of the NFMs.

Sample	DL, % (w/w)	TDL, %	Actual DL, μg	EE, %
zeinT-1PEO/3PCL	5.0	3.4	30.83 ± 1.03	75.49 ± 2.60
zeinT-25PCL	5.0	0.8	28.64 ± 1.64	82.49 ± 4.66
T25PCL	2.0	0.7	5.99 ± 0.02	70.36 ± 2.67

of T from pristine 25PCL fibers only reached 10 % over three days. The release of T from the NFMs was found to follow Higuchi kinetics (Table 4).

3.6. Biological studies

Inhibition of *E. coli* and *S. aureus* by T-loaded zein-1PEO/3PCL and zein-25PCL samples was comparable to the T disc control (Fig. 6**A**). Drug-free NFMs did not demonstrate inhibition zones. Viability of fibroblasts in the presence of zein-based NFMs was similar for zein-1PEO/3PCL and zein-25PCL samples and above 80 %, as measured using an MTT assay (Fig. 6**B**). This was further confirmed by the release of LDH from the cells, which did not exceed 5 % (Fig. 6**C**). Adhesion of fibroblasts was more pronounced on 25PCL NFMs as compared to zein-1PEO/3PCL, both with and without T (Fig. 7). The wound scratch assay demonstrated cell migration and rapid gap closure within 24 h in the

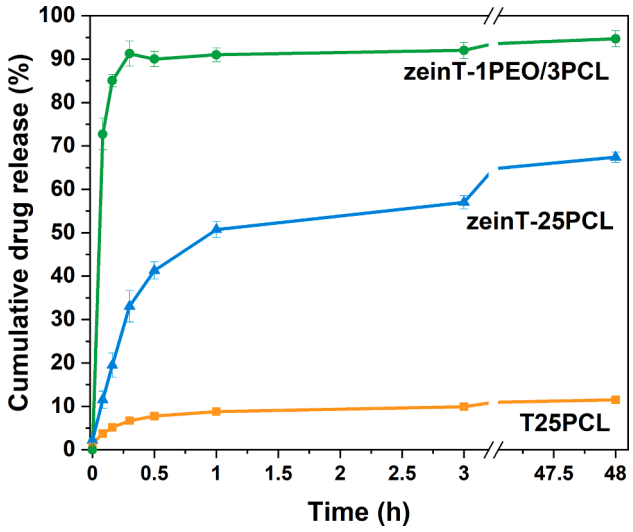

Fig. 5. Release of tetracycline hydrochloride from the NFMs.

Table 4
Release kinetics of T from the NFMs.

Sample	Model fitting		
	Zero order	First order	Higuchi
	R^2	R^2	R^2
zeinT-1PCL/3PEO	0.633	0.845	0.950
zeinT-25PCL	0.870	0.583	0.941
T25PCL	0.784	0.586	0.951

presence of all NFMs, with a slightly denser cell monolayer in the case of zein-25PCL NFMs (Fig. 8).

4. Discussion

Fiber diameter and distribution in wound dressings are essential for cell attachment and migration in the wound site as well as for gas exchange (Azimi et al., 2020; Liu et al., 2021). In comparison to our previously developed zein-PEO core–shell microfibers (Akhmetova et al., 2020), the zein-PCL core–shell fibers showed ~ 50 % smaller diameters, resulting with fibers in the nanofiber range (Fig. 1). This is advantageous for their use in wound dressings, as nanofibrous scaffolds have been found to enhance fibroblast attachment compared to microfibrous scaffolds due to their larger specific surface area (Bondar et al., 2008; Chen et al., 2009). The difference in fiber diameters compared to the fibers previously reported by us most likely is a consequence of the use of AA as a shell solvent in this study instead of aqueous ethanol. AA has a high boiling point of 118 °C and, therefore, displays a slower evaporation than aqueous ethanol, subsequently allowing more jet stretching before fiber solidification, resulting in smaller fiber diameters (Luo et al., 2012). However, electrospinning was more challenging with the gradual increase of PCL in the presence of PEO, which is most likely due to the immiscibility between PEO and PCL (Li et al., 2014; Qiu et al., 2003), as confirmed by the MDSC analysis that resulted in two separate peaks (Fig. 4**A**). The decreased fiber diameter of the core–shell fibers as compared to the control fibers from pristine PCL (Fig. 1) may further be due to the lower viscosity of zein solution (0.11 Pa s ± 0.01 Pa s) in comparison to the pristine PCL solution (20.28 Pa s ± 0.41 Pa s) that facilitated further elongation of the jet. This is in agreement with another study on multi-layer matrices containing zein and PCL (Alhusein et al., 2013). The bimodal distribution of T-loaded fibers that was observed at 25 % (w/v) PCL may be the result of a poor compatibility between the hydrophobic PCL and the hydrophilic drug T (Fig. 1). Similar compatibility issues between polymers and drugs have been reported previously (Chou et al., 2015; Haroosh et al., 2014; Karuppuswamy et al., 2015). Nevertheless, fabricating multimodally distributed fibers may be advantageous in terms of cell attachment and migration, as different cell types respond differently to different fiber diameters (Jenkins and Little, 2019; Sankar et al., 2017).

Retaining the structure of individual fibers and a high inter-fiber porosity in NFMs during application is essential to allow cell migration within the scaffold and to facilitate diffusion of nutrients and metabolites (Cai et al., 2017; Rnjak-Kovacina and Weiss, 2011). Water stability tests of our developed fibers revealed that the fibers best retain their morphology at high PCL concentrations (Fig. 1), likely an effect of the hydrophobicity of PCL (Siddiqui et al., 2018), as supported by the high contact angles of pristine 25PCL fibers with and without T (Fig. 2**A**). In contrast, samples containing PEO and only small amounts of PCL (zein-1PEO/1PCL and zein-1PEO/3PCL) did not retain their morphology (Fig. 1). This is most likely due to the hydrophilicity of PEO, which facilitates penetration of water molecules into zein, and the plasticizing effect of water on zein (Lawton, 2004). These results are in agreement with those obtained for zein-PEO microfibers developed earlier, which did not fully retain their shape for the same reasons (Akhmetova et al., 2020).

Wettability and water uptake are important to keep a moist environment for wound healing and to facilitate cell migration and attachment as well as diffusion of nutrients in the wound site (Azimi et al., 2020; Liu et al., 2021). With respect to the contact angle (wettability) measurements, which were carried out on dry NFMs, surface hydrophobicity/hydrophilicity of the fibers plays an important role. In the pristine PCL fiber mats, the contact angle was heavily influenced by the hydrophobicity of PCL (Siddiqui et al., 2018) and, therefore, stayed high and did not change over the short measurement period of 30 s, indicating a low wettability (Fig. 2**A**). In contrast, the decreasing contact angles and, hence, higher wettabilities of all core–shell fibers (Fig. 2**A**) may be due to partial mixing of the core and shell solutions occurring within the Taylor cone during electrospinning (Chou et al., 2015). Since both zein and T are soluble in AA (Li et al., 2011), such mixing may have taken place and resulted in the presence of zein or T in the shell of the

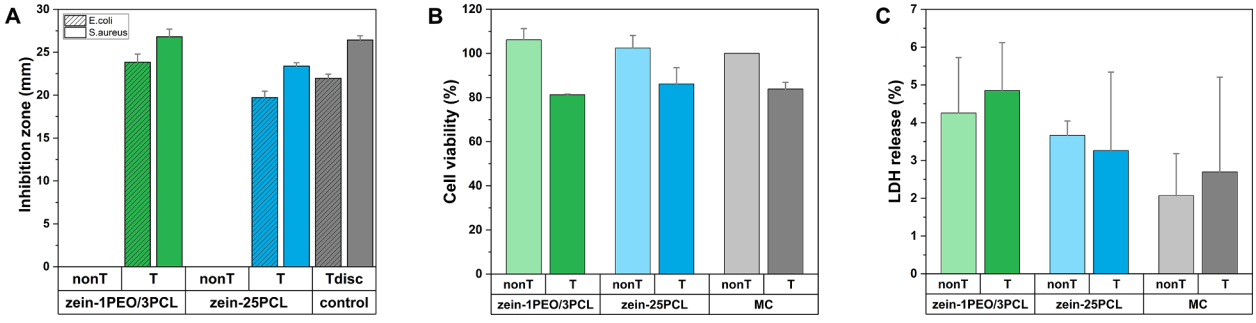

Fig. 6. Results for antimicrobial and cell viability studies. (A) Bacterial inhibition, (B) MTT assay and (C) LDH assay in the presence of different NFMs.

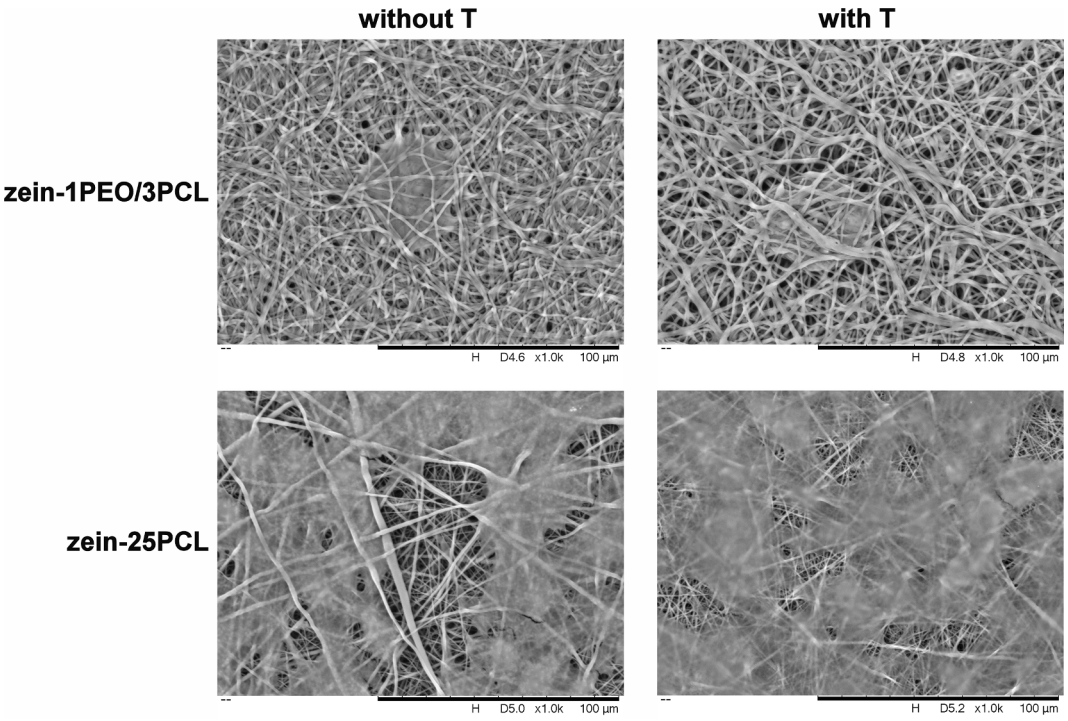

Fig. 7. Fibroblast cell adhesion on NFMs. Representative images were chosen.

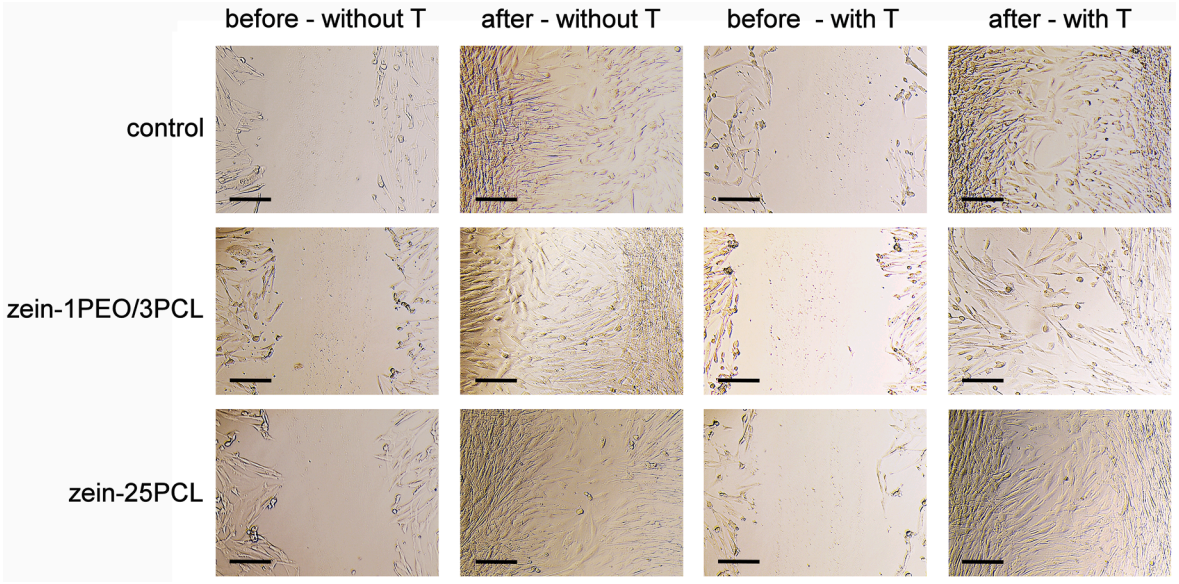

Fig. 8. Wound scratch assay in the presence of NFMs. Representative images were chosen. The scale bar represents 200 µm.

fibers. This in turn may have led to a higher surface hydrophilicity of the core–shell NFMs and, hence, a decreasing contact angle, which is consistent with a study on uniaxially electrospun PCL/zein fibers (Plath et al., 2021). In contrast, water uptake increased with increasing PCL concentration in the NFMs (Fig. 2**B**). Partial degradation of PCL induced by higher temperatures during electrospinning or in an acidic environment due to the use of AA may explain higher water penetration and absorption into pristine PCL and zein-25PCL scaffolds, an effect that may have unfolded over the incubation time of 48 h in water (Hernández et al., 2013; Ramazani and Karimi, 2014).

A wound dressing material should show ductility, high elasticity as well as a high tensile strength, allowing for an easy handling, comfortable wear as well as resistance against tear (Azimi et al., 2020). Upon examination of the core–shell NFMs in water, we found a clear change in mechanical properties depending on the shell composition (Table 2). While the mechanical properties of the dry PEO-containing NFMs reflect those of zein, which is brittle, stiff and shows low mechanical strength (Paliwal and Palakurthi, 2014; Shi et al., 2012), the increased elongation of the NFMs in a wetted state can be attributed to the water absorption by PEO and the subsequent plasticizing effect of water on zein (Lawton, 2004). In contrast, the mechanical properties of the PEO-free fiber mats are completely governed by the high ductility and low stiffness (high elasticity) of PCL (Baker et al., 2016; Urquijo et al., 2015), which was also confirmed by the stress–strain curves obtained in this study (Fig. 3).

In the PEO-containing NFMs, zein hydration and plasticization further resulted in a mass loss and shrinkage of the fiber mats (negative

shape retention) (Fig. 2**B**), which is in agreement with other studies involving electrospun zein (Alhusein et al., 2016; Xu et al., 2008), as well as flattening out of the fibers with partial loss of the fibrous structure (Fig. 1). The larger mass loss of PEO-containing fibers as compared to the NFMs without PEO most likely results from the solubility of PEO in water (Bailey and Koleske, 1976; Kianfar et al., 2021) and hence, partial erosion of the fibers. T-containing NFMs with PEO showed the largest mass loss (Fig. 2**B**) as a result of T release from the fibers, pore formation (Fig. 1) and subsequent enhancement of zein plasticization by water. The PEO-free NFMs further did not show mass loss or change in morphology (Fig. 2**B**), which is due to the hydrophobicity of PCL and its insolubility in water together with its high mechanical strength (Urquijo et al., 2015).

Sustained release of antibiotics from wound dressings can be beneficial to minimize their application frequency in clinical use and to prolong their antimicrobial effect. Our PCL-containing fibers display sustained T release with increasing PCL content and decreasing PEO content (Fig. 5). The burst release from PEO-containing fibers can be attributed to the hydrophilicity of PEO, which dissolves in water, leaving pores in the shell and facilitating diffusion of water into the zein core of the fibers and T diffusion out of the fibers (Bailey and Koleske, 1976; Kianfar et al., 2021). In contrast, hydration and hydrolytic degradation of the pristine PCL fibers and, hence, dissolution and release of T were significantly delayed due to the hydrophobicity of PCL, which is in accordance with our results on morphological and wettability characteristics as well as other studies (Alhusein et al., 2013; Bosworth and Downes, 2010; Karuppuswamy et al., 2015; Siddiqui et al., 2018). The best results in terms of sustained release were obtained for the zein-25PCL fibers with more hydrophilic surface properties, most likely due to the presence of zein and T in the shell of the fibers as a result of mixing between core and shell solutions during electrospinning as mentioned above (Plath et al., 2021). This led to a faster T release, which, however, was still delayed as compared to PEO-containing fibers.

The release kinetics from coaxially electrospun fibers are highly complex and are influenced by various factors such as drug loading, encapsulation efficiencies, morphological properties and solid-state properties (Chou et al., 2015). Our T-loaded zein-25PCL NFMs showed Higuchi release kinetics (Table 4) and, thus, represent systems characterized by diffusion-controlled T release without or with low surface erosion, showing potential for wound treatment (Dash et al., 2010). In the beginning, more T is released, which is present on or close to the surface of the fibers, followed by a diffusion-controlled release of T from within the fibers. Due to the slow degradation of PCL (Bosworth and Downes, 2010), bulk erosion of the PCL shell is unlikely in a short release study and is, thus, in agreement with the assumptions of the Higuchi release kinetics model (Chou et al., 2015; Karuppuswamy et al., 2015). For the PEO-containing fibers, we observed fiber swelling and erosion (Fig. 1), most likely associated with hydration as well as plasticization of the zein core. Even though their release follows the Higuchi model (Table 4), the observed burst release is likely to be a combination of mechanisms such as diffusion, swelling, structural cleavage and subsequent erosion.

Antimicrobial wound dressings should be able to release the loaded antibiotic in a controlled fashion and, thus, inhibit bacterial growth. They should also demonstrate biocompatibility and allow migration of fibroblasts, promoting wound healing (Liu et al., 2021). All drug-loaded fibers released T and inhibited the growth of both bacterial strains (Fig. 6**A**), showed good cytocompatibility (Fig. 6**B,C**) and allowed attachment of fibroblasts (Fig. 7). It can, hence, be concluded that they all have potential for tissue regeneration and wound healing purposes. A comparison of zein-1PEO/3PCL and zein-25PCL NFMs showed that fibroblasts attached more to and spread more out on the zein-25PCL samples (Fig. 7). This may be a result of starting surface degradation of PCL within the first 24 h of incubation and subsequent exposure of polar functional groups such as carboxyl and hydroxyl groups as well as generating a rougher fiber surface, all of which has previously been shown to increase the surface hydrophilicity of PCL fibers, the interaction with ECM molecules and consequently fibroblast attachment (Augustine et al., 2015; Kumar et al., 2012). The high tensile strengths of zein-25PCL scaffolds as compared to the PEO-containing fibers (Table 2) may be an additional advantage, providing good mechanical support and thereby allowing adhesion and migration of fibroblasts across the wound bed (Mondal et al., 2016). The wound scratch assay is a simple *in vitro* method, where a scratch in a confluent monolayer imitates an injury, leading to subsequent cell migration and wound closure (Alavarse et al., 2017). For both tested NFMs and the control, migration and proliferation of new fibroblasts in the scratch area were observed (Fig. 8). The dense cell monolayer, which formed after treatment with zeinT-25PCL fibers as compared to the control and zeinT-1PEO/3PCL indicates that zein-25PCL fibers show promising properties for wound healing through migration and proliferation, consistent with another study (Kouser et al., 2021).

5. Conclusion

In this study, we set out to improve the mechanical properties and alter the drug release behavior of our previously developed antimicrobial electrospun zein-PEO core–shell fibers by adding hydrophobic PCL, a polymer known for its ductility and elasticity, to the shell. We produced and compared zein-PCL core–shell fibers with and without additional PEO in the shell and used pristine PCL fibers as a reference. Overall, the zein-PCL core–shell fibers without PEO demonstrated the desired mechanical properties, i.e., water stability, ductility and mechanical strength. Moreover, we successfully altered the release behavior of the fibers from burst release of our zein-PEO fibers to a sustained release of tetracycline hydrochloride from the zein-PCL fibers and confirmed their antimicrobial activity. We further proved cytocompatibility as well as an enhanced fibroblast cell attachment on our zein-PCL fiber mats. In conclusion, the zein-PCL fibers contribute to the ongoing research on biodegradable wound dressings, which release the active ingredient in a sustained fashion.

Funding

This research was funded by LEO Foundation grants LF17063 (A.H.) and 2016–11-01 (A.H., M.v.d.P., M.M., J.C., A.M. and A.-L.S.).

CRediT authorship contribution statement

Alma Martin: Conceptualization, Investigation, Methodology, Data curation, Formal analysis, Validation, Writing – original draft. **Jun Cai:** Investigation, Methodology, Writing – review & editing. **Anna-Lena Schaedel:** Data curation, Formal analysis, Validation, Writing – review & editing. **Mariena van der Plas:** Data curation, Methodology, Writing – review & editing. **Martin Malmsten:** Conceptualization, Supervision, Writing – review & editing. **Thomas Rades:** Conceptualization, Supervision, Writing – review & editing. **Andrea Heinz:** Conceptualization, Data curation, Formal analysis, Funding acquisition, Validation, Supervision, Writing – review & editing.

Declaration of Competing Interest

The authors declare that they have no known competing financial interests or personal relationships that could have appeared to influence the work reported in this paper.

Acknowledgements

The authors would like to thank the Drug Delivery and Biophysics of Biopharmaceuticals group of the Department of Pharmacy, University of Copenhagen, for providing the pendant drop and HPLC equipment. Stine Harloff-Helleberg is thanked for help with the viscosity measurements.

References

EMA, 2021. Q3C (R8): Impurities: guideline for residual solvents. European Medicines Agency -Committee for Medicinal Products for Human Use, Amsterdam.

Agrawal, K.S., Sarda, A.V., Shrotriya, R., Bachhav, M., Puri, V., Nataraj, G., 2017. Acetic acid dressings: Finding the Holy Grail for infected wound management. Indian J. Plast. Surg. 50, 273–280.

Akhmetova, A., Lanno, G.M., Kogermann, K., Malmsten, M., Rades, T., Heinz, A., 2020. Highly Elastic and Water Stable Zein Microfibers as a Potential Drug Delivery System for Wound Healing. Pharmaceutics 12, 458.

Alavarse, A.C., de Oliveira Silva, F.W., Colque, J.T., da Silva, V.M., Prieto, T., Venancio, E.C., Bonvent, J.J., 2017. Tetracycline hydrochloride-loaded electrospun nanofibers mats based on PVA and chitosan for wound dressing. Mater. Sci. Eng. C Mater. Biol. Appl. 77, 271–281.

Alhusein, N., Blagbrough, I.S., Beeton, M.L., Bolhuis, A., De Bank, P.A., 2016. Electrospun Zein/PCL Fibrous Matrices Release Tetracycline in a Controlled Manner, Killing Staphylococcus aureus Both in Biofilms and Ex Vivo on Pig Skin, and are Compatible with Human Skin Cells. Pharm. Res. 33, 237–246.

Alhusein, N., Blagbrough, I.S., De Bank, P.A., 2013. Zein/polycaprolactone electrospun matrices for localised controlled delivery of tetracycline. Drug. Deliv. Transl. Res. 3, 542–550.

Augustine, R., Dominic, E.A., Reju, I., Kaimal, B., Kalarikkal, N., Thomas, S., 2015. Electrospun poly(epsilon-caprolactone)-based skin substitutes: In vivo evaluation of wound healing and the mechanism of cell proliferation. J. Biomed. Mater. Res. B Appl. Biomater. 103, 1445–1454.

Azimi, B., Maleki, H., Zavagna, L., De la Ossa, J.G., Linari, S., Lazzeri, A., Danti, S., 2020. Bio-Based Electrospun Fibers for Wound Healing. J. Funct. Biomater. 11, 67.

Bailey, F.E., Koleske, J.V., 1976. Chapter 4 - Solution properties of poly(ethylene oxide), Poly(ethylene Oxide). Academic Press.

Baker, S.R., Banerjee, S., Bonin, K., Guthold, M., 2016. Determining the mechanical properties of electrospun poly-epsilon-caprolactone (PCL) nanofibers using AFM and a novel fiber anchoring technique. Mater. Sci. Eng. C Mater. Biol. Appl. 59, 203–212.

Bondar, B., Fuchs, S., Motta, A., Migliaresi, C., Kirkpatrick, C.J., 2008. Functionality of endothelial cells on silk fibroin nets: comparative study of micro- and nanometric fibre size. Biomaterials 29, 561–572.

Bosworth, L.A., Downes, S., 2010. Physicochemical characterisation of degrading polycaprolactone scaffolds. Polym. Deg. Stab. 95, 2269–2276.

Cai, S.J., Li, C.W., Weihs, D., Wang, G.J., 2017. Control of cell proliferation by a porous chitosan scaffold with multiple releasing capabilities. Sci. Technol. Adv. Mater. 18, 987–996.

Chen, M., Patra, P.K., Lovett, M.L., Kaplan, D.L., Bhowmick, S., 2009. Role of electrospun fibre diameter andcorresponding specific surface area (SSA) on cell attachment. J. Tissue Eng. Regen. Med. 3, 269–279.

Chou, S.F., Carson, D., Woodrow, K.A., 2015. Current strategies for sustaining drug release from electrospun nanofibers. J. Control. Release 220, 584–591.

Dash, S., Murthy, P.N., Nath, L., Chowdhury, P., 2010. Kinetic modeling on drug release from controlled drug delivery systems. Acta Pol. Pharm. 67, 217–223.

Feng, X., Li, J., Zhang, X., Liu, T., Ding, J., Chen, X., 2019. Electrospun polymer micro/nanofibers as pharmaceutical repositories for healthcare. J. Control Release 302, 19–41.

Ghorbani, M., Mahmoodzadeh, F., Yavari Maroufi, L., Nezhad-Mokhtari, P., 2020. Electrospun tetracycline hydrochloride loaded zein/gum tragacanth/poly lactic acid nanofibers for biomedical application. Int. J. Biol. Macromol. 165, 1312–1322.

Han, D., Steckl, A.J., 2019. Coaxial Electrospinning Formation of Complex Polymer Fibers and their Applications. Chempluschem 84, 1453–1497.

Haroosh, H.J., Dong, Y., Lau, K.-T., 2014. Tetracycline hydrochloride (TCH)-loaded drug carrier based on PLA:PCL nanofibre mats: experimental characterisation and release kinetics modelling. J. Mater. Sci. 49, 6270–6281.

He, M., Jiang, H., Wang, R., Xie, Y., Zhao, C., 2017. Fabrication of metronidazole loaded poly (epsilon-caprolactone)/zein core/shell nanofiber membranes via coaxial electrospinning for guided tissue regeneration. J. Colloid Interface Sci. 490, 270–278.

Hernández, A.R., Contreras, O.C., Acevedo, J.C., Guadalupe, L., Moreno, N., 2013. Polycaprolactone Degradation Under Acidic and Alkaline Conditions. Am. J. Polym. Sci. 3, 70–75.

Janmohammadi, M., Nourbakhsh, M.S., 2019. Electrospun polycaprolactone scaffolds for tissue engineering: a review, International International Journal of Polymeric Materials and Polymeric. Biomaterials 68, 527–539.

Jenkins, T.L., Little, D., 2019. Synthetic scaffolds for musculoskeletal tissue engineering: cellular responses to fiber parameters. NPJ Regen. Med. 4, 15.

Jiang, H., Zhao, P., Zhu, K., 2007. Fabrication and characterization of zein-based nanofibrous scaffolds by an electrospinning method. Macromol. Biosci. 7, 517–525.

Kanjanapongkul, K., Wongsasulak, S., Yoovidhya, T., 2010. Investigation and Prevention of Clogging During Electrospinning of Zein Solution. J. Appl. Polym. 118, 1821–1829.

Karuppuswamy, P., Reddy Venugopal, J., Navaneethan, B., Luwang Laiva, A., Ramakrishna, S., 2015. Polycaprolactone nanofibers for the controlled release of tetracycline hydrochloride. Mater. Lett. 141, 180–186.

Kianfar, P., Vitale, A., Dalle Vacche, S., Bongiovanni, R., 2021. Enhancing properties and water resistance of PEO-based electrospun nanofibrous membranes by photo-crosslinking. J. Mater. Sci. 56, 1879–1896.

Kouser, S., Prabhu, A., Sheik, S., Prashantha, K., Nagaraja, G.K., D'Souza J, N., Navada, K.M., Manasa, D.J., 2021. Poly (caprolactone)/sodium-alginate-functionalized halloysite clay nanotube nanocomposites: Potent biocompatible materials for wound healing applications. Int. J. Pharm. 607, 121048.

Kumar, G., Waters, M.S., Farooque, T.M., Young, M.F., Simon, C.G., 2012. Freeform Fabricated Scaffolds with Roughened Struts that Enhance both Stem Cell Proliferation and Differentiation by Controlling Cell Shape. Biomaterials 33, 4022–4030.

Labib, G., 2018. Overview on zein protein: a promising pharmaceutical excipient in drug delivery systems and tissue engineering. Expert Opin. Drug Deliv. 15, 65–75.

Lawton, J.W., 2004. Plasticizers for Zein: Their Effect on Tensile Properties and Water Absorption of Zein Films. Cereal Chem. 81, 1–5.

Li, Y., Xia, Q., Shi, K., Huang, Q., 2011. Scaling behaviors of alpha-zein in acetic acid solutions. J. Phys. Chem. B 115, 9695–9702.

Li, Y.F., Rubert, M., Aslan, H., Yu, Y., Howard, K.A., Dong, M., Besenbacher, F., Chen, M., 2014. Ultraporous interweaving electrospun microfibers from PCL-PEO binary blends and their inflammatory responses. Nanoscale 6, 3392–3402.

Liu, X., Xu, H., Zhang, M., Yu, D.G., 2021. Electrospun Medicated Nanofibers for Wound Healing: Review. Membranes (Basel) 11.

Luo, C.J., Stride, E., Edirisinghe, M., 2012. Mapping the Influence of Solubility and Dielectric Constant on Electrospinning Polycaprolactone Solutions. Macromolecules 45, 4669–4680.

Luraghi, A., Peri, F., Moroni, L., 2021. Electrospinning for drug delivery applications: A review. J. Control. Release 334, 463–484.

Maharjan, B., Joshi, M.K., Tiwari, A.P., Park, C.H., Kim, C.S., 2017. In-situ synthesis of AgNPs in the natural/synthetic hybrid nanofibrous scaffolds: Fabrication, characterization and antimicrobial activities. J. Mech. Behav. Biomed. Mater. 65, 66–76.

Memic, A., Abudula, T., Mohammed, H.S., Joshi Navare, K., Colombani, T., Bencherif, S. A., 2019. Latest Progress in Electrospun Nanofibers for Wound Healing Applications. ACS Appl. Bio. Mater. 2, 952–969.

Mondal, D., Griffith, M., Venkatraman, S.S., 2016. Polycaprolactone-based biomaterials for tissue engineering and drug delivery: Current scenario and challenges. Int. J. Polym. Mater. Polym. Biomater. 65, 255–265.

Moreira, J., Vale, A.C., Alves, N.M., 2021. Spin-coated freestanding films for biomedical applications. J. Mater. Chem. B 9, 3778–3799.

Olsson, M., Jarbrink, K., Divakar, U., Bajpai, R., Upton, Z., Schmidtchen, A., Car, J., 2019. The humanistic and economic burden of chronic wounds: A systematic review. Wound Repair Regen. 27, 114–125.

Op 't Veld, R.C., Walboomers, X.F., Jansen, J.A., Wagener, F., 2020. Design Considerations for Hydrogel Wound Dressings: Strategic and Molecular Advances. Tissue Eng. Part B Rev. 26, 230-248.

Pachuau, L., 2015. Recent developments in novel drug delivery systems for wound healing. Expert Opin. Drug Deliv. 12, 1895–1909.

Paliwal, R., Palakurthi, S., 2014. Zein in controlled drug delivery and tissue engineering. J. Control. Release 189, 108–122.

Pedram Rad, Z., Mokhtari, J., Abbasi, M., 2018. Fabrication and characterization of PCL/zein/gum arabic electrospun nanocomposite scaffold for skin tissue engineering. Mater. Sci. Eng. C Mater. Biol. Appl. 93, 356–366.

Pedram Rad, Z., Mokhtari, J., Abbasi, M., 2019. Calendula officinalis extract/PCL/Zein/Gum arabic nanofibrous bio-composite scaffolds via suspension, two-nozzle and multilayer electrospinning for skin tissue engineering. Int. J. Biol. Macromol. 135, 530–543.

Plath, A.M.S., Facchi, S.P., Souza, P.R., Sabino, R.M., Corradini, E., Muniz, E.C., Popat, K. C., Filho, L.C., Kipper, M.J., Martins, A.F., 2021. Zein supports scaffolding capacity toward mammalian cells and bactericidal and antiadhesive properties on poly (ε-caprolactone)/zein electrospun fibers. Mater. Today Chem. 20, 100465.

Qiu, Z., Ikehara, T., Nishi, T., 2003. Miscibility and crystallization of poly(ethylene oxide) and poly(ε-caprolactone) blends. Polymer 44, 3101–3106.

Ramazani, S., Karimi, M., 2014. Investigating the influence of temperature on electrospinning of polycaprolactone solutions. e-Polymers 14, 323–333.

Rnjak-Kovacina, J., Weiss, A.S., 2011. Increasing the pore size of electrospun scaffolds. Tissue Eng. Part B Rev. 17, 365–372.

Sankar, S., Sharma, C.S., Rath, S.N., Ramakrishna, S., 2017. Electrospun Fibers for Recruitment and Differentiation of Stem Cells in Regenerative Medicine. Biotechnol. J. 12, 1700263.

Selling, G.W.W., Woods, K.K., Biswas, A., 2011. Electrospinning formaldehyde-crosslinked zein solutions. Polym. Int. 60, 537–542.

Selling, G.W.W., Woods, K.K., Sessa, D., Biswas, A., 2008. Electrospun Zein Fibers Using Glutaraldehyde as the Crosslinking Reagent: Effect of Time and Temperature. Macromol. Chem. Phys. 209, 1003–1011.

Shi, K., Yu, H., Lakshmana Rao, S., Lee, T.C., 2012. Improved mechanical property and water resistance of zein films by plasticization with tributyl citrate. J. Agric. Food Chem. 60, 5988–5993.

Siddiqui, N., Asawa, S., Birru, B., Baadhe, R., Rao, S., 2018. PCL-Based Composite Scaffold Matrices for Tissue Engineering Applications. Mol. Biotechnol. 60, 506–532.

Trucillo, P., Di Maio, E., 2021. Classification and Production of Polymeric Foams among the Systems for Wound Treatment. Polymers (Basel) 13.

Urquijo, J., Guerrica-Echevarría, G., Ignacio Eguiazábal, J., 2015. Melt processed PLA/PCL blends: Effect of processing method on phasestructure, morphology, and mechanical properties. J. Appl. Polym. Sci. 132, 42641.

Xu, W., Karst, D., Yang, W., Yang, Y., 2008. Novel zein-based electrospun fibers with the water stability and strength necessary for various applications. Polym. Int. 57, 1110–1117.